Inglis, G.N., Rohrssen, M., Kennedy, E.M., Crouch, E.M., Raine, I.J., Strogen, D.P., Naafs, B.D.A., Collinson, M.E and Pancost, R.D. **Terrestrial methane cycle perturbations during the onset of the Paleocene–Eocene Thermal Maximum**.

Supplementary Information

The following supplementary information includes text, figures and datasets.

The dataset, which is uploaded separately, contains two tables:

Table 1: Bulk and compound specific carbon isotope data for Otaio River
Table 2: GDGT distributions and temperature proxies for Otaio River
Table 3: Lipid biomarker thermal maturity parameters at Otaio River

Additional methodology

We analysed 24 samples from Otaio River, including both lignite and nearshore shallow marine interbeds (Supplementary Information). Approximately 0.5-10 g of sediment were extracted via Soxhlet apparatus for 24 hours using dichloromethane (DCM):methanol (MeOH) (2:1 v/v) as the organic solvent. The total lipid extract (TLE) was then separated over alumina into apolar and polar fractions using hexane:DCM (9:1 v/v) and DCM:MeOH (1:2 v/v, respectively). Urea adduction was performed upon the apolar fraction to separate into non-adduct (i.e. cyclic) and adduct (i.e. aliphatic) fractions. To achieve this, 200 µl of hexane, 200 µl of acetone and 200 µl of urea (10% in MeOH) were successively added to the saturated hydrocarbon fraction. The sample was frozen for ca. 60 min until urea crystals formed. Solvent was then removed under a gentle stream of N_2 and the urea extracted (×5) with ca. 1 ml of *n*-hexane (cyclic fraction). The urea crystals were then dissolved in 500 µl of MeOH and 500 µl of water and the aliphatic fraction was extracted (×5) with ca. 1 ml of *n*-hexane. The adduction procedure was repeated on the adduct fraction once more to ensure all non-adduct material was removed.

The adduct and non-adduct fraction was analysed via gas chromatographymass spectrometry (GC-MS) using a Thermo Scientific ISQ Single Quadrupole gas chromatography-mass spectrometer. Using helium as the carrier gas, 1 µl of sample (dissolved in hexane) was injected at 70 °C using an on-column injector. The temperature program included four stages: 70 °C hold for 1 min, 70–130 °C at 20 °C/min rate; 130–300 °C at 4 °C/min; and temperature hold for 20 min at 300 °C. The electron ionisation source was set at 70 eV. Scanning occurred between *m/z* ranges of 50–650 Daltons. The GC was fitted with a fused silica capillary column (50 m × 0.32 mm i.d.) coated with a ZB1 stationary phase (dimethylpolysiloxane equivalent, 0.12 µm film thickness). Compounds were identified based upon published spectra, characteristic mass fragments and retention times (e.g. Inglis et al. 2018 and ref. therein).

The non-adduct and adduct fraction was also analysed via gas chromatographycombustion-isotope ratio mass spectrometry (GC-C-IRMS) using an Isoprime 100 GCcombustion-isotope ratio mass spectrometer system. Samples were measured in duplicate with a reproducibility of <0.5‰ and $\delta^{13}C$ values were converted to

VPDB by bracketing with an in-house gas (CO_2) of known $\delta^{13}C$ value. The Instrument stability was monitored by regular analysis of an in-house standard; long-term precision is ± 0.3‰.

Injection volume was 1 µl onto to a Zebron-I nonpolar column (50 m × 0.32 mm i.d., 0.10 µm film thickness). GC conditions were the same as described above for GC-MS analysis. The polar fraction, containing the GDGTs, was dissolved in hexane/*iso*-propanol (99:1, v/v) and passed through 0.45µm PTFE filters. Fractions were analysed by high performance liquid chromatography/atmospheric pressure chemical ionisation – mass spectrometry (HPLC/APCI-MS) [34]. Normal phase separation was achieved using two Waters Acquity UPLC BEH Hilic (2.1×150mm; 1.7 µm i.d.) with a flow rate of 0.2 ml min^{-1} Samples were eluted isocratically with 78% A and 18% B for 25 min followed by a linear gradient to 35% B over 25 min, then a linear gradient to 100% B in 30 min, where A=hexane and B=hexane:IPA (9:1, v/v). Analyses were performed in selective ion monitoring mode (SIM) to increase sensitivity and reproducibility and M+H+ (protonated molecular ion) GDGT peaks were integrated.

Branched GDGT paleotemperature calibration

Land air temperature (LAT) exerts a strong control on the methylation of brGDGTs, whereby higher LATs are associated with decreasing methylation (De Jonge et al., 2014, Peterse et al., 2012, Weijers et al., 2007). For lignites (TOC > 30%) and coastal marine sediments (TOC < 10%), we translate MBT_{5ME} vales (Figure S2) into LAT using a Bayesian calibration (Crampton-Flood et al., 2020) using a global soil and peat dataset (Naafs et al., 2017, De Jonge et al., 2014). We employ the $BayMBT_0$ model which calibrates the MBT'_{5Me} index to the average temperature of all months that have an average temperature above 0°C. The prior mean (15°C) is based on existing palynofloral temperature estimates (Pancost et al., 2013).

Thermal maturity indicators

Thermal maturation can influence brGDGT distributions (Schouten et al. 2013). Thermal maturation can be assessed using the distribution of hopanoid isomers, where samples with low ββ/(σβ+βσ+ββ) indices (< 0.5) indicate elevated thermal maturation. In our section, C_{27-32} hopane ββ/(σβ+βσ+ββ) indices range between 0.3 and 0.7 (average: 0.5).This implies low-to-moderate thermal maturation. This is consistent with other lines of evidence, which suggest low-to-moderate thermal maturity at Otaio Gorge. This includes: i) an abundance of leaves, pollen and plant cuticle, ii) the lack of 'extended' hopane isomers (i.e. C_{32} to C_{35} 17α,21β(H) isomers), and iii) high carbon preference indices (average: 6.1; Figure S3).

Figure S1: Branched glycerol dialkyl glycerol tetraethers used to calculate MBT', CBT and related indices. 6-methyl branched GDGTs denoted by a dash

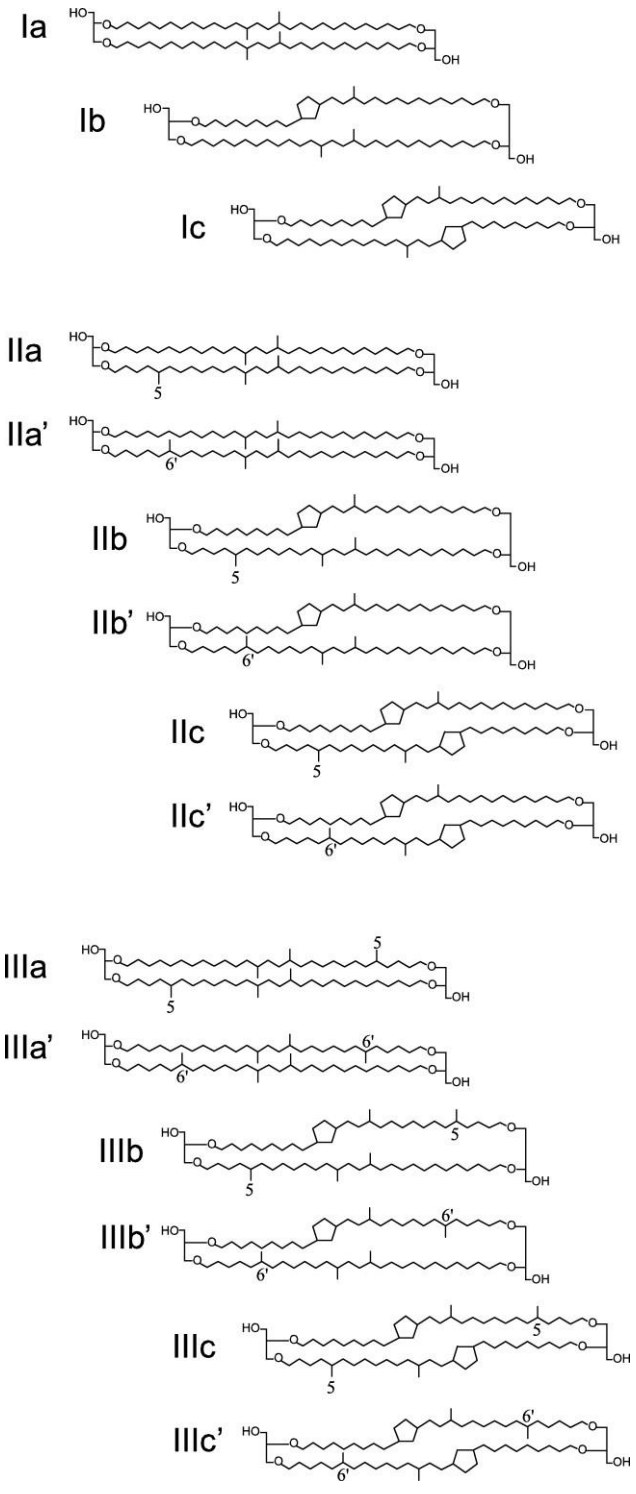

Figure S2: MBT_{5Me} values within the Otaio River section. A) MBT_{5ME} in lignite seams, b) MBT_{5ME} in marine interbeds.

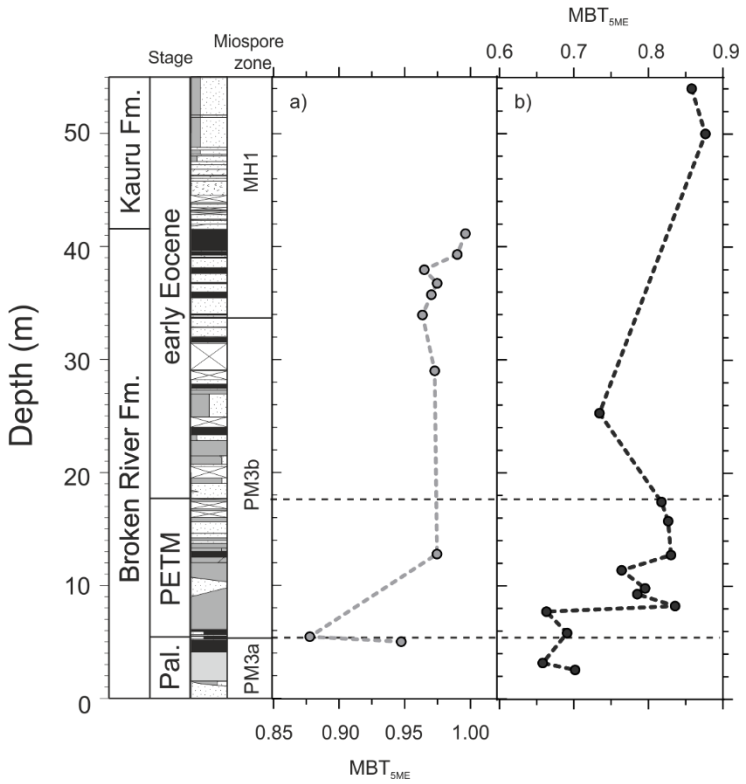

Figure S3: Thermal maturity indicators within the Otaio River section. a) Carbon Preference Index (CPI) (Naafs et al., 2019), b) C_{27} to C_{32} hopane ββ/(ββ+αβ+βα) ratio